Statistical environment representation for navigation in natural environments

Stefan Rolfes* **Maria-João Rendas****

I3S CNRS URA 1376, Université de Nice Sophia Antipolis
2000, Route des lucioles; Les Algorithmes; Bat. Euclide B
06903 Sophia Antipolis - Cedex
France

Abstract

In this paper we present a novel approach to mobile robot navigation based on environment representation by statistical models. Natural unstructured scenes are interpreted as realisations of *Random Closed Sets* (RCS), whose global characteristics are mapped. Contrary to the feature based approach, this environment representation does not require the existence of outstanding objects in the workspace, and is robust with respect to small dynamic changes. We address the relocalisation problem assuming that a statistical model, serving as a map of the environment, is available a priori. Simulation results demonstrate the feasibility of our approach.

1 Introduction

In the recent years a variety of navigation methods for autonomous mobile robots have been studied. While good results have been obtained, in particularly for indoor robots, a lot of open issues still need to be addressed. This is especially true for navigation in natural highly unstructured environments. While terrestrian robots can use GPS for localisation, an autonomous vehicle operating underwater (AUV) has to strongly rely on its perceptual capabilities in order to estimate its position.

The main challenge of navigation in large underwater areas concerns the safety of the robot: if it looses track of its current position autonomous recovery can no longer be guaranteed. To overcome the problems associated with search and recovery, the vehicle needs to be able to return to a *homing area* (e.g. the vicinity of the boat from which it was launched), where it can be picked up after completion of the mission. If the positioning error becomes too large, the robot will miss the homing area and get lost.

Navigation of AUV's requires thus that the estimation error be maintained below appropriate bounds. This cannot be guaranteed if the vehicle relies only on proprioceptive (inertial) sensors. Perceptual data must be used to find natural landmarks that can be periodically used for relocalising the robot.

The most common approach for relocalisation of mobile robots is feature based, see e.g. [1, 2]. Features, described by low dimensional parameter vectors, are stored in an internal map. Relocalisation is subsequently done by estimating the rigid motion that matches recently observed features to those already contained in the map.

While the feature based approach yields good results in environments where dense maps of outstanding features, that can be easily identified, can be built, it is less suited to unstructured environments where unstable feature identification leads to frequent mismatch or to absence of feature matches. We propose a novel environment description that is suited for environments where identification of salient features is difficult.

Instead of creating a detailed description of the environment as a collection of features, we propose a representation by statistical models that capture the local macroscopic characteristics of unstructured

* Email: rolfes@i3s.unice.fr
** Email: rendas@i3s.unice.fr

environments. Such characteristics can be (i) the number of objects per unit area, (ii) their spatial distribution, and/or (iii) the distribution of basic local morphological attributes, such as shape, color or size. The advantage of this representation is that it does not rely on individual features. Mismatch problems are thus eliminated, and the representation is robust to perturbations (small displacement of objects, or shape deformations).

The paper is organized as follows. In section 3 we propose to model the robot's environment as a realization of a *Random Closed Set* model. In section 2 we discuss environment descriptions in general terms and propose in section 3 the use of RCS models as suitable descriptions for unstructured environments. Section 4 gives an overview of how RCS models can be used for mobile robot navigation. We assume here that such a description is available a-priori and do not address here the problem of joint mapping and localization for these models. In section 5 we present preliminary simulation results that validate our approach. Finally, some conclusions are drawn in section 6.

2 Environment descriptions

An exhaustive description of natural unstructured environments is not necessary for the purpose of mobile robot navigation. The basic criteria for the choice of suitable environment maps are (i) simplicity of coding and (ii) robustness of recognition. The choice of the map depends thus of the nature of the envionment in which the robot progresses. In general we can induce a partition of the robot's workspace by associating to each point a mark belonging to a limited number of classes $\mathcal{M}$. Indoor environments can e.g. be classified into : 'corridors', 'walls', 'doors', etc. For outdoor environments plausible classes are for example : 'stones', 'sand', 'tree', etc. This is a rather coarse classification, but still adequate for navigation if the classes are choosen in an appropriate way. This classification, based on the perceptual data (using e.g. sonars or cameras), induces a series of patches on the workspace of the robot. This discretized description of the environment can be mathematically represented as the union of compact sets:

$$\Xi = \bigcup_{i=1}^{\infty} (\Xi_i + p_i, m_{j_i})), \quad \Xi_i \in \mathcal{K}, \quad m_{j_i} \in \mathcal{M}. \tag{1}$$

In the equation above $\mathcal{K}$ is a family of compact sets (set of possible shapes) and $\mathcal{M}$ is the mark space, designating the class to which the set belongs (other attributes than shape). Without loss of generality, we assume that the center of gravity of the sets Ξ_i is at the origin. The sum $\Xi_i + p_i$ denotes the set Ξ_i translated by the vector $p_i \in \mathbb{R}^2$. The Ξ_i represent thus the morphological characteristics of the objects (or patches) and p_i their location in the workspace. An example is shown in figure 1. Figure 1(a) shows a raw images of the sea bottom, where the white regions of the image correspond to dead 'Maerl' (coraline alga) found at the Orkney islands in the north of Scotland. This image shows well the patchy nature of this natural field. The classified version of this image ($\mathcal{M}$ contains just one class) is illustrated in figure 1(b).

Commonly used approaches for environment description are e.g. the grid based and the feature based approach. Using the grid based approach (e.g. using the classes 'occupied' and 'free space') we obtain directly Ξ. The disadvantages are the storage capacities required, particularly problematic for large scale environments. The second approach is the feature based approach. An environment description is obtained by creating a geometric description of the Ξ_i and their locations p_i. If the morphological characteristics of the individual objects are simple (e.g. structured indoor environments) the feature based approach is well suited, since the complexity of feature matching is reduced. Both approaches, however, are very sensitive to errors in the classification of the raw data.

In unstructured environments the patches have arbitrary shapes and relocalisation using the feature based approach tends to fail, due to the increasing complexity involved in the matching process. A different way to describe unstructured environments, by considering that the patches form a random pattern can be formulated using the notion of **random closed set** (RCS) models.

3 Modelisation of scattered objects as random closed sets

Random closed sets are mathematical models that are appropriate for modelisation of random-like patterns. They have been frequently used in biological and physical contexts, in order to analyze natural patterns.

One of its earliest applications was the modelisation of the crystallization in metals by Kolmogorov in 1937 [3]. Good introductions to this formalism can be found in [4, 5].

A random closed set Ξ (a collection of randomly shaped compact sets, as given by equation (1)) is a doubly stochastic process, also called germ-grain model. A first random point process describes the spatial location of objects (germs), denoted by p_i in equation 1, at which realizations of a second stochastic process (grains) determine the local morphology of the field, i.e. the characteristics of the sets Ξ_i. For this model we can assume that the intersection between distinct patches can be non empty. The distribution of the germs can, for example, be clustered, structured or uniformly distributed, see figure 2.

(a) (b) (c)

Fig. 1. (a) Image from the sea-bottom taken in the north of scotland. The white patches correspond to crystalized (dead) coral 'Maerl'. (b) The image after classification. (c) A modelisation using a clustered distribution (clusters of varying size composed of compact discs with random radius.

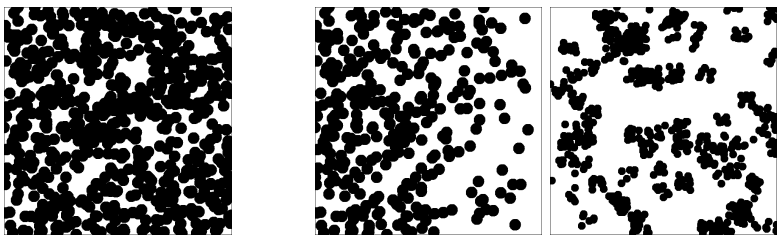

(a) (b) (c)

Fig. 2. Examples of RCS models. (a) isotropic boolean model (uniformly distribution of the patches), (b) anisotropic boolean model, the number of patches depends on the location, (c) a clustered distribution of the patches.

We assume that the counting measure μ associated to the point process (germ model) is a member of a parameterized family of distributions G_p:

$$\mu \in G_p = \{\mu_\lambda, \lambda \in \Lambda\},$$

where Λ is a compact set. The vector λ is the collection of parameters that determine the statistical distribution of the locations p_i. The shape process (grain model) constrains the set of possible elementary shapes (e.g. to discs of random radius, lines of random orientation or to mixtures of them). Similarly to the germ process we consider that the distribution of the shapes can be parameterized by a finite number of parameters γ, such that

$$\kappa \in G_{\Xi_0} = \{\kappa_\gamma, \gamma \in \Gamma\},$$

where κ is a probability measure over the space of possible shapes, Γ is a compact set and Ξ_0 is a random shape. Different model types can be obtained by considering distinct pairs of families G_p, G_{Ξ_0} (for instance,

for G_p: homogeneous Poisson point process, regular pattern, etc., and for G_{Ξ_0}: discs whose radii are uniformly distributed in an interval, line segments of random length and orientation, etc.). The random closed set model is thus given by the model type $M_{i,j} = (G_p^{(i)}, G_{\Xi_0}^{(j)})$. A particular model $M \in M_{i,j}$ is specified by the parameter vector $\theta = (\lambda, \gamma)$, $M(\theta) = \mu_\lambda, \kappa_\gamma$, where $\mu_\lambda \in G_p^{(i)}$ and $\kappa_\gamma \in G_{\Xi_0}^{(j)}$.

The aim of the theory of random closed sets is to determine the model type $M_{i,j}$ and the model parameter $\hat{\theta})(\hat{\lambda}, \hat{\gamma})$, such that an observed scene (inside an observation window (OW) of size $\nu(OW)$, where $\nu(.)$ is the Lebesgue measure) is a typical realization of the random closed set model $M(\theta) = \mu_\lambda, \kappa_\gamma \in M_{i,j}$. It is often difficult to obtain direct counting measures and estimates of the morphological characteristics of the sets Ξ_i from classified images, especially when the elementary grains Ξ_i can overlap, as illustrated in figure 2. Estimation of the distributions of the germ and the grain processes by direct identification of each individual shape is in these cases impossible.

We exploit here an important property of random closed sets [6], stating that the distribution of any general random closed set is uniquely determined by the *hitting capacity* which is, for each compact set K, the probability that the intersection of K with the RCS Ξ is not empty:

$$T_\Xi(K) = P(\Xi \cap K \neq \emptyset); \quad \forall K \in \mathcal{K}, \tag{2}$$

where $\mathcal{K}$ is the family of all compact sets. The important fact is that knowledge of the hitting capacities for all $K \in \mathcal{K}$ is **equivalent** to the knowledge of the model parameter θ (assuming the model type to be known). In the case of isotropic models (θ is independent of the location and orientation of the observer) we know that $T_\Xi(K) = T_\Xi(K + p)$, where $K + p$ is the set K translated by the vector p. Under the assumption that the RCS model is locally isotropic (inside the observation window WO) we can obtain empirical estimates of the hitting capacities from classified images.

For obvious reasons (limited computational capacities) we are able to estimate hitting capacities only for a finite collection of compact sets $K^n = \{K_1, \ldots, K_n\}$. In this case we capture just a limited number of characteristics of Ξ. Consequently, the sets K_i should be choosen in order to capture those that are the most relevant. We call K^n the structuring elements (notation proposed by [7]).

For some model types we can find analytical forms of equation (2), allowing us to compute the hitting probabilities in terms of the model parameters θ. This is the case for the well studied **Boolean model**. The germ process is a Poisson point process, determined by the intensity parameter λ, and the grains are i.i.d. realisations of compact sets. The hitting capacity for boolean models can be shown (see [4]) to be

$$T_\Xi(K) = 1 - exp(-\lambda \mathbf{E}_\kappa(\nu(\Xi_0 \oplus \check{K}))), \tag{3}$$

where $\oplus$ is the Minkowski-addition ($(A \oplus B) = \{a + b; \forall a \in A, b \in B\}$), $\mathbf{E}(.)$ is the statistical expectation operator and $\check{K} = \{-x; x \in K\}$. For many models it is theoretically possible to find an equivalent boolean model. If we assume e.g. a cluster process, whose cluster locations are determined by a Poisson point process, we can consider the clusters as being very complex shaped grains. The hitting capacities can be obtained by (3). The main difficulty, however, is to compute $\mathbf{E}_\kappa(\nu_d(\Xi_0 \oplus \check{K}))$. In this case a non boolean model can be more convenient.

In this presentation of our approach to mobile robot navigation we concentrate on modelisation by Boolean models. Ongoing work concerns characterization of other types of random closed set models as those illustrated in figure 2, in particular clustered models, which seem good candidates to describe some kinds of natural scenes.

In general, the perceptual characteristics change throughout the workspace, induced by varying temperature, soil fertility, ocean current, etc. If these variations are abrupt, we can partition the workspace into disjoint areas A_k (see figure 3), whose macroscopic characteristics are described by different types of statistical models $M_{i_k,j_k}(\theta)$:

$$\text{Workspace} = \bigcup_{k=1}^{\infty} A_k, \quad A_k \leftrightarrow M^k(\theta) \equiv M_{i_k,j_k}(\theta) = (\mu_\lambda^{(i_k)}, \kappa_\gamma^{(j_k)}),$$

with $\mu_\lambda^{(i)} \in G_p^{(i)}$ and $\kappa_\gamma^{(i)} \in G_{\Xi_0}^{(i)}$. We denote by $M^k(\theta)$ the model associated to area A_k. To model smooth variations of the field inside each region A_k, we let the model parameter θ depend on the location x

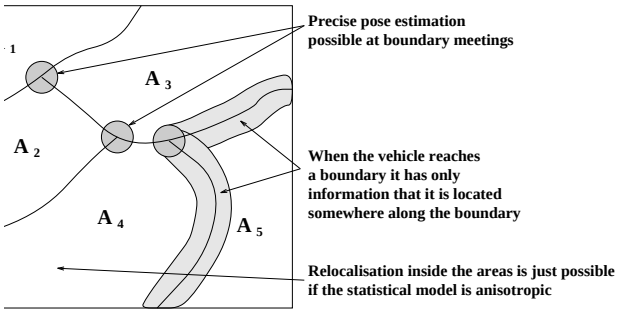

Fig. 3. Segmentation of the workspace into areas where the characteristics of the environment are described by different random closed set models.

$$\text{Map:} \quad x \to \theta(x) = (\lambda(x), \gamma(x)); \quad x \in A_k. \tag{4}$$

The approach to navigation of robots in natural environments proposed here considers that the map given in the previous equation has been learned by (or given a priori to) the robot, i.e., the robot knows the partition $\{A_k\}$ and the piecewise continuous vector field defined by (4).

4 Mobile robot navigation based on RCS models: a Bayesian approach

We address now the problem of using the map defined in the previous section to estimate the robot location. We consider first local navigation inside each region A_k and start the discussion with a simple example. If the model parameter $\theta(x)$ is known for all $x \in A_k$, the inverse map $\theta^{-1} : \theta \to \mathcal{B} \cap A_k$, where $\mathcal{B}$ is the field of all Borel sets of the ambient space, can be computed. If $\theta^{-1} = A_k$ the model M_{i_k,j_k} is *isotropic* and *relocalisation* inside A_k is not possible. If, however, $\theta^{-1} = B \subset A_k$ (a strict subset), the model is *anisotropic* and the vehicle's pose, after observation of θ, can be restricted to locations in B. An example of an isotropic scene was given in figure 2(a), and of an anisotropic scene in figure 2(b).

In the isotropic case, relocalisation is only possible on the boundaries between adjacent areas, indicated by an abrupt change of the model type or by an abrupt change of the model parameters. It is thus convenient to perform the partitioning $\{A_k\}$ of the workspace such that the boundaries indicate not only a change of the model type but also abrupt changes of the model parameters.

Navigating between adjacent areas requires thus hypothesis testing in order to determine the correct model type and to determine when the robot crossed the boundaries. Such hypothesis testing can be done using available tools for model selection, such as Generalized Maximum Likelihood, MDL [8] or the AIC criteria [9]. We illustrate here just navigation inside smooth anisotropic areas ($\theta(x)$ continuous), assuming that the model type has been correctly determined. In order to obtain a pose estimate we use a Bayesian approach.

We assume here that the dynamic model of the robot's state X_k is known:

$$X_k = f(X_{k-1}) + g(u_{k-1}) + w_k,$$

where $f(.)$ is a known (non-linear) function, $f : \mathcal{C} \to \mathcal{C}$, where $\mathcal{C}$ is the configuration space of the robot's state, w_k is a white noise and u_k is a driving term. The optimal MMSE estimate of the robot's state X_k, given the past observations $Y^k = \{Y_1, \ldots, Y_k\}$, is given by the conditional mean

$$\hat{X}_k = \int_{\mathcal{X}} X_k p(X_k|Y^k) dX_k,$$

where $p(X_k|Y^k)$ is the a posteriori density of the robot's state, given the observations. The a posteriori density $p(X_k|Y^k)$ can be updated by alternating prediction and filtering steps:

$$p(X_{k-1}|Y^{k-1}) \overset{Pred.}{\to} p(X_k|Y^{k-1}) \overset{Filt.}{\to} p(X_k|Y^k).$$

The prediction step (convolution) propagates the probability distribution in the state space according to the dynamic model. If Y_k is the output of a memoryless observator, the filtering step (pointwise multiplication) computes

$$p(X_k|Y^k) \propto p(X_k|Y^{k-1})p(Y_k|X_k).$$

The observations $Y_k = (D_k, Z_k)$ contain proprioceptive observations D_k (velocity, heading,...) and measures Z_k, obtained using perceptual sensors (vision, sonar,...). The measures Z_k are in our case estimates of the hitting capacities for the structuring elements $K^n = \{K_1, \ldots, K_n\}$. These estimates are obtained directly from the images (classified) acquired at time k: $Z_k \equiv \hat{T}_k = \{\hat{T}_k(K_1), \ldots, \hat{T}_k(K_n)\}$. If we assume that the proprioceptive and the perceptual observations are uncorrelated we obtain:

$$p(Y_k|X_k) = p(D_k|X_k)p(\hat{T}_k|\theta(X_k)),$$

since the observations $\hat{T}_k$ depend on X_k only through the parameters of the RCS model at that point. In order to use an optimal filter we need to identify correctly the conditional density $p(\hat{T}_k|\theta(X_k))$. Since the uncertainty of the empirical estimates $\hat{T}_k$ depends on the size of the observation window, we should rewrite the conditional density as $p(\hat{T}_k|\theta(X_k), \nu(OW))$ - the larger the observation window the better are our estimates of the hitting capacities. This density is in general not gaussian.

The equations above define the general framework of navigation using a Bayesian approach. In the actual state of the work we are restricted to boolean models for which we were able to derive analytical expressions for the conditional density (for a single structuring element). In order to apply the approach to real data we still need to spend an effort on the analysis of different appropriate models.

We characterised $p(\hat{T}|\theta, \nu(OW))$ for locally isotropic boolean models. An estimate $\hat{T}$ of the hitting capacities can be obtained by placing the compact set (the structuring element) K at a number N (sampling number) of random positions $\{p_i\}_{i=1}^N$ inside the observation windows and evaluate at each time the event: K hits (or not) Ξ:

$$H_N = \{h(p_i)\}_{i=1}^N; \quad h(p_i) \in (0, 1).$$

The estimated value $\hat{k}_{hit} = \sum_{i=1}^N h(p_i)$ denotes the number of times that Ξ was hit by K. If we assume that all events $h(p_i)$ are mutually independent the probability law of k_{hit} is binomial:

$$p(k_{hit}|N) = \binom{N}{k_{hit}} \hat{T}^{k_{hit}}(1-\hat{T})^{N-k_{hit}},$$

where $\hat{T} = \hat{k}_{hit}/N$ is the estimated hitting capacity. The variance of $p(k_{hit}|N)$ is $\sigma_k^2 = N\hat{T}(1-\hat{T})$. An open (currently under study) problem is to determine the maximum sampling number N^* for which the hitting events are independent. This number depends on the size of the observation window, the structuring element and the RCS model: $N^* = f(\nu(OW), K, \theta)$. The determination of N^* requires a more detailed analysis of the RCS model. Here we state just that if N is choosen too small the uncertainty of the estimates (given by the variance σ_k^2) is very large, but the probability of k_{hit} is truely determined by the binomial distribution. If N is choosen too large the events are no longer independent and the distribution of k_{hit} is no longer binomial. This is illustrated in figure 4(a,b), showing the empirical probability distributions for different values of N ($N = 30$ and 100). The empirical distributions were obtained by simulating an isotropic boolean model (the grains are compact discs whose radii are uniformly distributed in (r_1, r_2)) and an observation window was placed at random positions (20000 positions). The plots show also the corresponding binomial distributions which for $N = 30$ approximate well the empirical distribution (the events can be considered to be independent) which is not the case for $N = 100$.

For large N (number of samples per image) the binomial distribution tends to a Gaussian, as shown in figure 4. The density $p(\hat{T}_k|\theta(X_k), \nu(OW))$ is approximately Gaussian: $\mathcal{N}(\hat{k}_{hit}/N, \hat{T}(1-\hat{T})/N)$. In this case we can propagate the a posteriori density of the robot state given the past observations by an Extended Kalman Filter (EKF), whose computational complexity is low. In pratice we see that this approximation is good even for relatively small N if the hitting capacities T are close to 0.5 (figure 4(a)). In extreme situations were T is close to 0 or 1 (figure 4(c)) the approximation becomes worse. Such situations occur in particular when the intensity of the germ process is very small (for small sized grains). We overcome this problem partly by selecting a structuring element K (having an appropriate size) resulting in a hitting capacity close

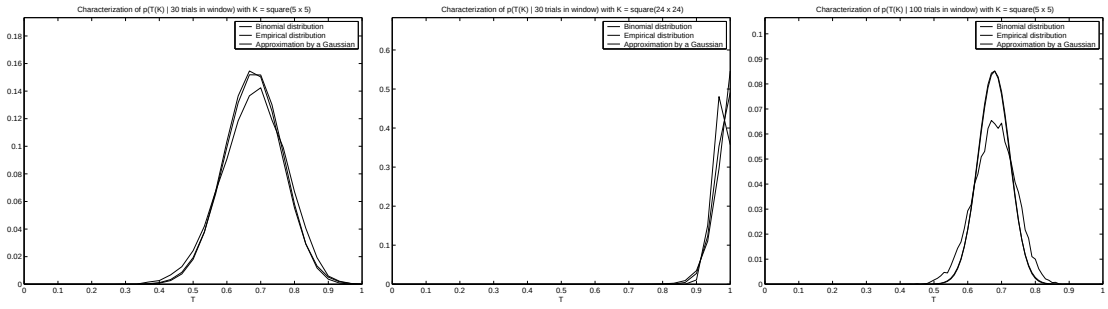

(a) (b) (c)

Fig. 4. Empirical probabilities of the hitting capacities (based on 20000 estimates of k_{hit} for an isotropic model), along with the binomial distribution and its approximation by a Gaussian. (a) number of samples per image: N = 30 (structuring element K square of sidelength 5), (b) N = 30 (structuring element K square of sidelength 24), and (c) N = 100. (structuring element K square of sidelength 5).

to 0.5. However,increasing the size of the structuring element reduces the number of samples N for which the hitting events are independent.

In addition, we required the consecutive observations to be uncorrelated. This is true when two consecutive observation windows do not intersect. In practice this condition is only verified if the perceptual observations are used periodically, dependent on the speed of the vehicle. If we use the perceptual information permanently we need to reduce either the number of samples N or alternatively enlarge the uncertainty of the observations. Let α be the percentage of the image that corresponds to new observations. If we assume that the number N is linearly dependent on the size of the observation window we set:

$$p(\hat{T}_k|\theta(X_k), \nu(OW)) \hat{=} \mathcal{N}(\hat{k}_{hit}/N, \hat{T}(1-\hat{T})/(N\alpha)). \tag{5}$$

5 Results

We present in this section results that demonstrate the feasibility of mobile robot navigation based on environment descriptions by random closed set models. We simulated the navigation of an underwater robot equipped with *proprioceptive* sensors (compass and speed sensor) that are used for dead-reckoning and a camera pointing at the sea bottom. The robot moves at a constant altitude in an environment that was obtained by sampling from an anisotropic Boolean model. The patches are compact discs whose radii are uniformly distributed in an interval, $r \in [r_1, r_2]$. While the shape process is constant allover the workspace we let the intensity λ, of the point process (Poisson distributed), depend on the location x. The map of the environment is thus given by

$$\theta(x) = (\lambda(x), r_1, r_2), \quad x \in [-440, 1500] \times [-600, 1400].$$

We tested the approach for two different intensity maps $\lambda_i(x); i = 1, 2$ that are illustrated in figure 5(a) (figure 5(b) shows the realisations of the corresponding environments Ω_i (the locations of the patches) along with the initial location of the robot and the position estimate (with an initial error $(+30, +20)$). The ellipse indicates the initial uncertainty and the square indicates the area that is locally observed by the camera (some "observations" are shown in figure 6).

We point out that a feature based approach is not well suited for this kind of environments: no single salient perceptual feature can be easily identified in the environment (due to the large number of patches and their similar shapes), resulting in a very complex pattern matching process, which is, at the same time, highly sensitive to small perturbations.

A simulated (non-modeled) ocean current (of magnitude $\simeq 3$) perturbates the nominal trajectory of the robot, resulting in an important drift between the true position and its dead-reckoning estimate. Throughout the trajectory images are acquired at regular time intervals. The perceptual observations are empirical estimates of the hitting capacity $Z_i = \{\hat{T}_i(K_1)\}$ for a single structuring element K_1 (square of side length d), that are directly obtained from the images based on a fixed number $N = 30$ of samples.

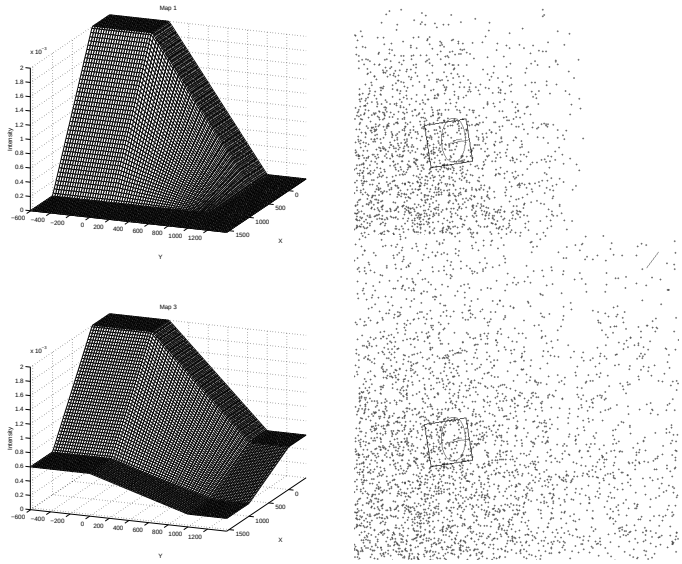

(a) (b)

Fig. 5. (a) Intensity maps $\lambda_1(x); i = 1, 2$; (b) Corresponding realisations of the environment. Each environment contains areas in which the model is anisotropic (no relocalisation possible).

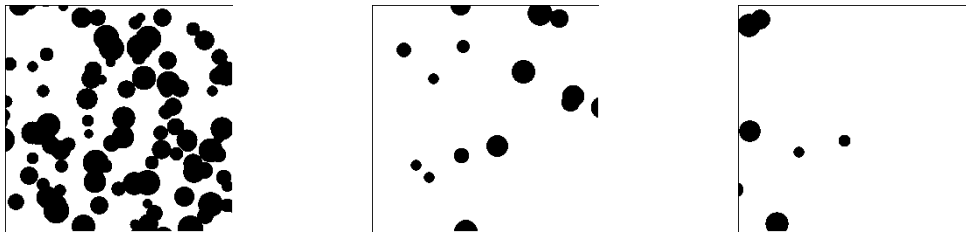

Fig. 6. Local observations at different positions.

The probability density $p(Z_i|\theta(X_k))$ (derived from a binomial distribution for isotropic models) was approximated by a Gaussian density (according to the discussion in the previous section). In order to take into account that the consecutive observations are correlated we fixed the factor α of equation (5) as a function of the translational speed.

We fixed an arbitrary trajectory, that was used for all simulations. For each of the intensity maps we performed several simulations, each for a different realisation of the environment. The estimated trajectory (dotted line) obtained for a single simulation based on map $\lambda_1(x)$ is shown in figure 7(a), along with the true trajectory. An estimated trajectory that is merely based on odometry (without using perceptual observations) is shown in figure 7(b). The final positioning errors, illustrated by the arrows, show clearly the gain of the RCS map-based navigation compared to dead-reckonin estimates.

The performance of the map based navigation is better illustrated by figure 8. Figures 8(a) and (c) show the positioning error (absolute distance) and the extension of the uncertainty ellipse (2σ) in direction of the true robot position for simulations based on the maps $\lambda_i(x); i = 1, 2$ respectively. For both maps we obtained estimates that are consistent with the positioning uncertainty (Similar results were obtained for different realisations of the environment). Figure 8(b) and (d) show the evolution of the robot's pose where we assumed that the consecutive observations are uncorrelated. The resulting uncertainty of the robot's state is too optimistic. The pose error is no longer consistent with the positioning uncertainty. While for these results the pose error remains bounded this can in general not be guaranteed (The EKF diverges).

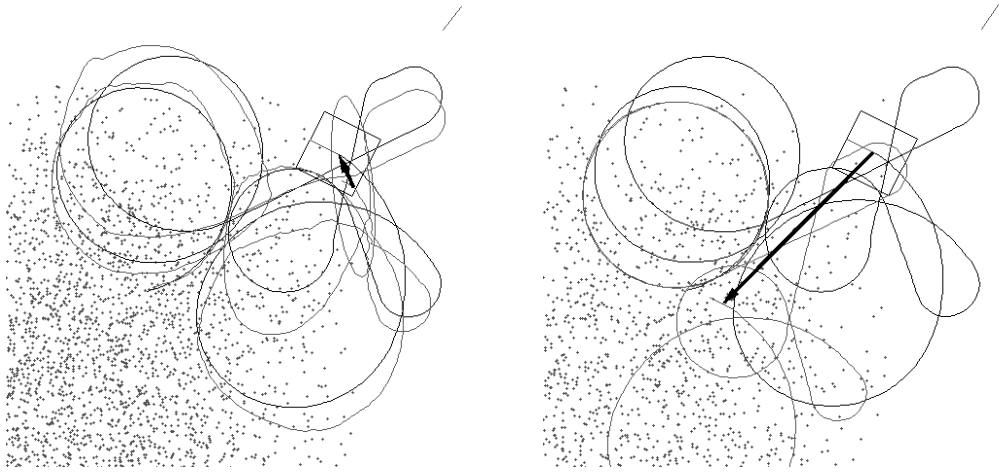

(a) (b)

Fig. 7. (a) Navigation result for map $\lambda_1(x)(observationsuncorrelated)$. (b) Position estimate is based merely on proptioceptive data (heading and speed measures). The thick error indicates the final positioning error.

The results illustrate also that the evolution of the size of the principal uncertainty support depends on the spatial distribution and the shape of the objects. If we compare the plots of figure 8(a) and (c) we see that the uncertainty of the robot's state is larger in the second environment. The evident reason is that the variations of the intensity are stronger in map λ_1 than in map $\lambda_2(x)$.

6 Conclusions

In this paper we proposed a novel environment description for robot navigation, using the formalism of random closed set models. These models capture the principal characteristics of an environment and do not rely on individual feature description. Knowledge of exact location (or shapes) of features is not required, resulting in increased robustness with respect to small changes. We present approximate expressions that enable definition of an approximation to the Bayesian estimator of the robot state for these models. The feasibility of the approach is demonstrated by simulation results.

A series of open problems must still be studied more thoroughly. In particular, we need to address the problem of identification of the correlation of hitting capacities for distinct structuring elements. Another open issue concerns the use of more complex RCS models, in order to describe clustered or regular environments. Analytical expressions need to be found for these models and the associated hypothesis testing formulated in order to discriminate between different types of regions. Finally the problem of joint mapping and localization for this kind of environment representations must be addressed in order to realize fully autonomous progression of a robot in a priori unknown environments: the robot must be able to simultaneously estimate the map (the model type along with the model parameter) and its position, using the autonomously created map.

Acknowledgments

This work has been partially funded by the European Union through the IST project SUMARE (IST-1999-10836, Survey of Marine Resources) and the Esprit/LTR project NARVAL (LTR-20185, Navigation of Autonomous Robots via Active Environment Perception).

References

1. J.A. Castellanos, J.M. Martinez, Neira J., and Tardós J.D., "Simultaneous Map Building and Localization for Mobile Robots: A Multisensor Fusion Approach," in *IEEE Proc. of the Int. Conf. on Robotics and Automation*, May 1998.
2. H.J. Feder, J.J. Leonard, and C.M. Smith, "Adaptive Mobile Robot Navigation and Mapping," *Int. Journal of Robotics Research*, July 1999.
3. A.N. Kolmogoroff, "Statistical theory of crystallization of metals," in *Bull. Acad. Sci. USSR Mat. Ser. 1*, 1937, pp. 355–359.

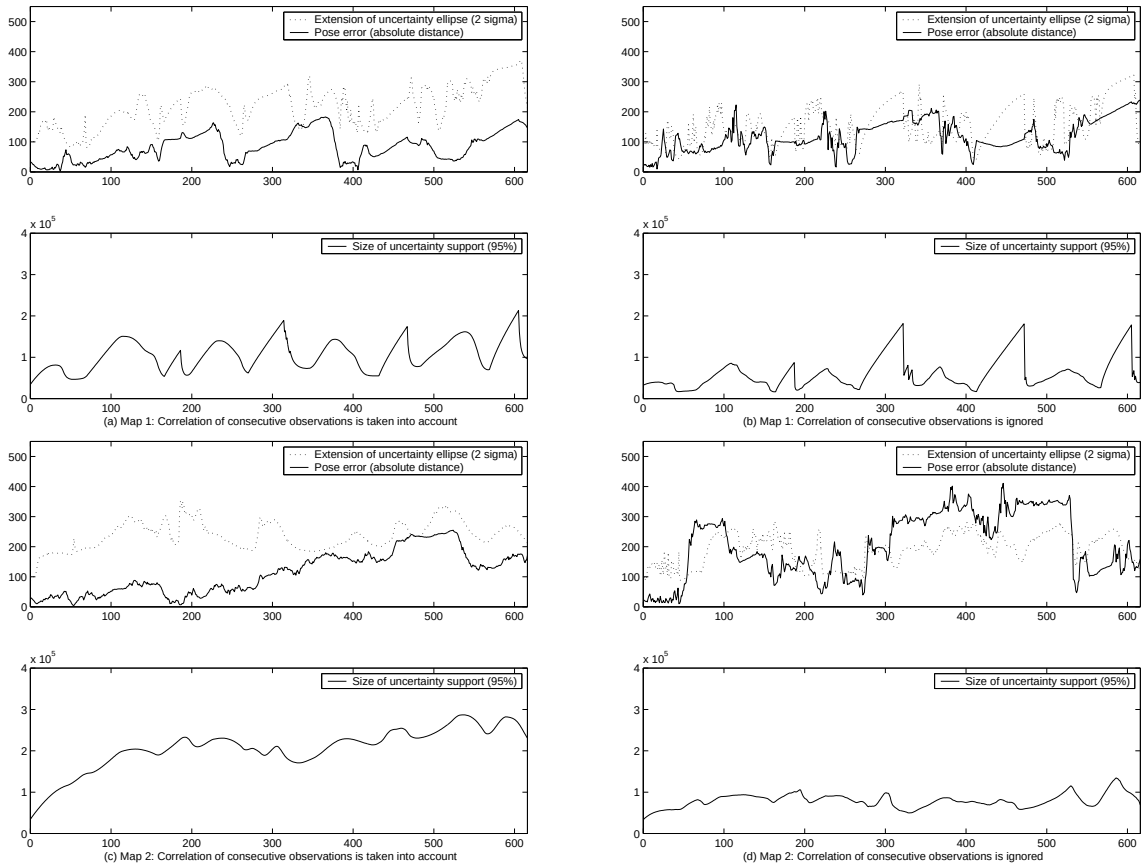

Fig. 8. Evolution of the position error during navigation in the two simulated environments and of the uncertainty support.

4. D. Stoyan, W.S. Kendall, and J. Mecke, *Stochastic Geometry and its Applications*, John Wiley & Sons, 1995.
5. O.E. Barndorff-Nielsen, W.S. Kendall, and M.N.M. van Lieshout, *Stochastic Geometry, Likehood and Computation*, Chapman & Hall/CRC, 1999.
6. G. Matheron, *Random Sets and Integral Geometry*, John Wiley and Sons, New York, 1975.
7. J. Serra, *Image Analysis and Mathematical Morphology*, Academic press, New York, 1982.
8. J. Rissanen, *Statistical Complexity in Statistical Enquiry*, World Scientific, 1989.
9. H. Akaike, "A new look at statistical model identification," in *IEEE Trans. Autom. Control*, 1974, vol. 19, pp. 716–723.

This article was processed using
the TEX macro package with SIRS2001 style